Rare earth elements recovery from secondary wastes by solid-state chlorination and selective organic leaching

S. Pavón[1,2], T. Lorenz[1,3], A. Fortuny[2], A.M. Sastre[4], M. Bertau[1]

[1]*Institute of Chemical Technology, TU Bergakademie Freiberg, Leipziger Straße 29, 09599 Freiberg, Germany*

[2]*Chemical Engineering Department, EPSEVG, Universitat Politècnica de Catalunya, Víctor Balaguer 1, 08800 Vilanova i la Geltrú, Spain*

[3]*Institute of Low-Carbon Industrial Processes, DLR German Aerospace Center, Walther-Pauer-Straße 5, 03046 Cottbus, Germany*

[4]*Chemical Engineering Department, ETSEIB, Universitat Politècnica de Catalunya, Diagonal 647, 08028 Barcelona, Spain*

ABSTRACT

Processing of end-of-life products (EoL) containing rare earth elements (REE) has gained increasing importance in recent years with the aim of avoiding supply risks. In addition, circular economy renders complete recirculation of technology metals mandatory. Fluorescent lamp wastes are an important source for REE recovery since they contain significant amounts, up to 55 wt. %, of Y and Eu in red phosphors. For these purposes, solid-state chlorination (SSC) is an economically attractive alternative to wet acid leaching treatment, which profits from a considerable reduction of chemicals consumption and process costs. Chlorination takes place with dry $HCl_{(g)}$ produced from thermal decomposition of $NH_4Cl_{(s)}$, not only converting the REE content of the Hg-free phosphor waste into water soluble REE metal chlorides, but also avoiding the implications of aqueous complex chemistry of REE. To establish an industrial process viable on a commercial scale, the SSC process has been optimized by (i) using a design of experiment (DOE) varying temperature, residence time, and g_{NH4Cl}/g_{solid} ratio and (ii) improved leaching of the chlorinated metals with an organic mixture selective for REE. As a result, 95.7% of the Y and 92.2% of the Eu were selectively recovered at 295.9 °C, 67 min and a ratio of 1.27 g_{NH4Cl}/g_{solid}, followed by quantitative selective leaching of the REE. Owed to its low chemicals consumption and operation costs, the current process allows for valorizing lamp waste even when raw material prices are low.

Keywords

Chlorination; Electronic waste; Fluorescent powder; Rare earths recovery; Recycling

1. Introduction

The recovery of rare earth elements (REE) from fluorescent lamp waste is an increasingly important issue considering the large number of devices sold and disposed of every year (Saratale et al., 2020). For instance, in 2019 0.9 Mt of lamp wastes were produced worldwide (Forti et al., 2020) While glass, metal and plastic fractions are recovered commercially, end-of-life (EoL) phosphors till now are not recycled. As a consequence of an economic process lacking, 0.2 Mt of phosphors with an average REE content of 23% were disposed of in landfills in Europe in 2017 (Swain and Mishra, 2019). The European Union alone is facing an annual growth rate for WEEE of 7% (Forti et al., 2020) In view of their amount expectedly reaching 52.2 Mt WEEE in 2021, a WEEE Directive has been established which promotes recycling and reuse instead of disposal (Alvarado-Hernández et al., 2019). In addition, as an outcome of banning traditional incandescent bulbs, the manufacture of fluorescent lamps has witnessed constant growth in the last years (Pavón et al., 2018). However, as of 1st September 2021, the 2009 and 2012 EU regulations regarding energy labelling and eco-design requirements will be replaced (European Commission, 2012, 2009a, 2009b). Most halogen lamps and traditional fluorescent lamps will be phased out as of September 2023 and replaced by modern lutetium aluminum garnet (LAG) LED lamps (European Commission, 2020). This development will inevitably result in a considerable waste stream reaching the recycling markets, which however, to a large proportion lack suitable REE recovery processes. The situation is aggravated by low REE commodity prices, which render almost all recycling activities uneconomical. Consequently, an effective and economically viable REE recycling technology is required, which takes into account the pricing pressure of the REE commodity markets.

An important issue in this context is the mercury content of the phosphor powders, without which fluorescent lamps do not work. While mechanical separation is established to recover aluminum end caps, plastics, glass and circuit boards, mercury content remains an issue. At present, dry and wet technologies are mainly used for Hg removal (Park and Rhee, 2016). Dry technology removes mercury by distillation, while wet methods use an absorbent prior to oxidizing and separating mercury.

REE recovery from waste streams has gained importance markedly, what is owed to their growing demand for advanced technologies (Li et al., 2020; Wu et al., 2018). Yet, the global REE market is small and opaque (Gutiérrez-Gutiérrez et al., 2015), what is directly linked to the 70.5% of global annual production of 120,000 t being concentrated in China (U.S. Geological Survey, 2020; Yang et al., 2019). It is obvious, that REE recovery from discarded lamps is essential to safeguarding the raw material base of the European industry.

There have been plentiful research activities on REE recycling processes (Ahn et al., 2020; Pavón et al., 2018). In particular, they are dealing with REE recovery from magnets, nickel-metal hydride batteries or fluorescent lamps (R. G. Saratale et al., 2020; Su et al., 2018)

because they represent > 80% of the RE market in terms of value (Hasegawa et al., 2018). However, despite the large number of studies, REE recovery from EoL fluorescent lamp waste is not conducted on an industrial scale, because the technology readiness level (TRL) typically does not exceed 6 or 7 (Innocenzi et al., 2014). Falling REE commodity prices in the years after 2011 and non-uniform waste streams make the situation even worse. To give an example, FNE Entsorgungsdienste Freiberg GmbH, a small enterprise in Freiberg, Saxony operates the MagnetoRec-process for spent FeNdB- and CoSm-magnets (Lorenz and Bertau, 2020, 2019) which with its half-tonne-per-day-scale is the largest REE-magnet recycling process outside China. This fact speaks for itself and vividly emphasizes the vital interest of the European Union in domestic REE recycling.

From the chemistry of fluorescent lamp phosphors, hydrometallurgical approaches appear most promising. These routes commonly commence with an acid digestion step (Wu et al., 2018), which however is cost-intensive and ineffective from a chemicals consumption point of view. Moreover, acid digestion requires an acid excess to work, for which reason the material stream is highly acidic, once the leaching step is done. To allow for REE precipitation or further processing of the digestion solution, the pH value must be increased or even neutralized. This process step generates even more cost intensive consumption of alkaline chemicals, what in turn in form of a salt freight produces another additional waste stream. To tackle these obstacles, an unconventional method such as the solid-state chlorination (SSC) is emerging as an alternative process, which has been proven to be more efficient and cheaper for the extraction and processing of metals (Bertau et al., 2015, 2014). This type of chlorination process refers to the conversion of the metal content of the primary or secondary raw material into water-soluble metal chlorides by the addition of chloride salts, such as $NaCl_{(s)}$, $CaCl_{2(s)}$ and $NH_4Cl_{(s)}$ (Mu et al., 2020). It had turned out in previous investigations, though, that energy consumption is an important process cost factor. This issue can easily be solved by using $NH_4Cl_{(s)}$, for which a lower temperature between 250 and 300 °C was shown sufficient (Lorenz and Bertau, 2020, 2019). The obtained metal chlorides are well soluble in water and can easily be reduced (Xing et al., 2020). Recent examples, where SSC has successfully been applied are the removal of copper and sulphur from copper slags at 1,200 °C with a residence time of 60 min, 0.14 mass ratio of $CaCl_2$/copper slag and an oxygen flow rate of 0.3 L/min (Li et al., 2018). Others treat primary REE ores (Okabe et al., 2020). In the Freiberg lab, Y and Eu were recovered from waste phosphor by treating with NH_4Cl and subsequent leaching with water (Lorenz et al., 2015). This method, known as the SepSELSA process, went into industrial application in 2015 (Bertau et al., 2014). To the best of our knowledge, this is the only process of its kind that is operated commercially. 27 tons of phosphor have been processed since. Other approaches work at higher temperature (400 °C, 2 h), yet lower yield (87.35%) after adding oxalic acid and subsequent calcination (Yu et al., 2016).

Owing to the successful application of SSC in REE recycling, the question was how the process can be optimized. The new process scheme focusing on an SSC process combined with a second selective organic leaching step (Leaching 2) is depicted in Fig. 1.

The main improvements addressed in this work are:

(i) **RE recycling process:** A second leaching (L2) was previously carried out through adding 2 M HNO_3 to recover REE (Pavón et al., 2019). However, the SSC process provides several advantages over acid leaching such as a decreased demand for chemicals, the avoidance of any strongly acidic wastewater and the implementation of the zero-waste concept. REE recovery was optimized by design of experiments (DOE) that allows for determining the global optimum yields depending on the different factors considered.

(ii) **RE selective leaching:** Instead of using acetic acid buffer or water (Lorenz and Bertau, 2017), a 2,4 pentanedione/ethanol mixture was used. The REE enriched liquor (Fig. 1) can be processed directly by solvent extraction technique in order to separate the individual REE. There is no precipitation interfering with the process.

(iii) **Chemicals costs:** The approach described in this work is compared to classic wet acid treatment by estimating of chemicals demand and costs.

In summary, REE recovery from EoL fluorescent lamp waste has been improved substantially through applying SSC. The subsequent selective organic leaching stage selectively separates REE from accompanying metals, such as Ca, P, Na, Sr.

2. Material and methods

2.1. Starting material

Fluorescent lamp waste was supplied as a fine, Hg-free powder by Recyberica Ambiental S.L. (Madrid, Spain). The waste was introduced to a first leaching step utilizing 1 M HNO_3 (Pavón et al., 2019). The $solid_{L1}$ obtained after filtration was used as the starting material. Its composition was determined by atomic emission spectrometry with inductively coupled plasma (ICP-OES, Optima 4300 DV, Perkin Elmer, MA, USA) after treatment with aqua regia at 90 ± 2 °C for 2 h in duplicate. Hg content was analyzed by cold vapor atomic absorption spectrometry (CV-AAS, Pye Unicam, Model SP9, Cambridge, UK) to verify that the samples were Hg-free. Particle size measurement was done by laser diffraction analysis (MasterSize 3000, Malvern Panalytical, United Kingdom).

2.2. Experimental set-up

Solid state chlorination (SSC) was conducted in a rotary kiln with a tubular inert gas connection made of quartz glass to prevent corrosion (Lorenz and Bertau, 2020, 2019). Samples were placed in the center of the glass tube between two tappers. Excess $NH_{3(g)}$ produced from NH_4Cl decomposition was funneled into a scrubbing bottle with glass wool to remove solid particles and absorbed in a second scrubbing bottle containing deionized water.

2.3. Preliminary tests

In order to properly define the levels of the factors (temperature, residence time and $g_{NH4Cl}/g_{solidL1}$ ratio) in the statistical design of experiments (DOE), different preliminary tests were carried out. Thermogravimetric analysis (TGA) and differential thermal analysis (DTA) were conducted (TGA/DSC 1, Mettler Toledo, OH, USA) to examine how REE yield depends on the temperature. TGA and DTA were carried out by mixing 1 g of $solid_{L1}$ with 1 g of $NH_4Cl_{(s)}$ and heating the mixture from 30 to 500 °C at a rate of 10 K/min. Three series of experiments were conducted with the following SSC conditions:

i) 60 min, 1 $g_{NH4Cl}/g_{solidL1}$ ratio and temperature range comprised from 250 to 325 °C
ii) 300 ºC, 1 $g_{NH4Cl}/g_{solidL1}$ ratio and a range of NH_4Cl:$solid_{L1}$ ratio from 0.5 to 3
iii) 300 ºC, 1 $g_{NH4Cl}/g_{solidL1}$ ratio and residence time from 30 to 120 min

The chlorinated solids, obtained after SSC at 300 °C and 325 °C, were analyzed by Infrared spectroscopy (FTIR-Spectrometer Nicolet iS10 by Thermo Fisher Scientific, MA, USA) and X-ray powder diffraction (Bruker D5000 by Bruker Corporation, MA, USA) to clarify and propose the reactions involved in the SSC and leaching steps.

2.4. Box Behnken design

Unlike recently reported investigations (Lorenz and Bertau, 2020, 2019), the mass of the leaching solution was not considered as a factor because the organic solution is not suitable for leaching metals from the unchlorinated waste material. The organic solution does not affect REE yield as long as the volume is sufficient to fully dissolve all metal chlorides. Therefore, SSC process and leaching stages have been optimized separately.

All experiments and their respective parameters are listed in Table 1. The software utilized for statistical evaluation was Statgraphics v.18 (Statpoint Technologies, VA, USA), which allows for determining the model equations describing how REE yields depend on the factors and correlations. Furthermore, the global optimum of REE yields can be predicted.

2.5. Solid-state chlorination

The mixture of 1 g of $solid_{L1}$-$NH_4Cl_{(s)}$ was introduced in the quartz tube of the rotary kiln. After deoxygenation flushing with $N_{2(g)}$ at 350 mL/min for 30 min at 2 rpm, the kiln was heated to the

reaction temperature specified in Table 1 at a heating ratio of 10 K/min and it was kept constant for 30 till 90 min. When the reactor was cooled to room temperature, the chlorinated residue was transferred to a beaker by rinsing the quartz tube with the organic leaching solution.

2.6. Leaching solution

The leaching solution was prepared by dissolving 5 mL of 2,4-pentanedione (99%, Alfa Aesar, MA, USA) in ethanol (ACS grade, Sigma-Aldrich, MO, USA) yielding a solution of 50 mL. The chlorinated residue was introduced into the organic leaching solution and stirred at room temperature for 30 min. The suspension was filtered through a PTFE membrane (0.2 µm, Filtrak, Germany) at 200 mbar. After addition of 50 mL 0.01 M HNO_3, the mixture of 2,4-pentanedione/ethanol was removed under ambient pressure at elevated temperature (T > 90 °C), yielding 50 mL leachate as nitrate. The organic leaching solution was collected to be reused in further leaching processes. Metal compositions were analyzed by ICP-OES.

3. Results and discussion

3.1. Starting material

Table 2 gives an average composition of lamp phosphors. Since YOX, Eu doped Y_2O_3, is the major constituent, Eu and Y alone account for 96.4 wt. % of total REE content. With less than 4 % in sum, the recovery of Ce, Gd and La appears hardly cost-effective, especially in view of the present price situation. The green and blue phosphors containing these REE are acid resistant, what renders their recovery tedious and costly. For this reason, the present work focuses solely on the recovery of Y and Eu. Since the lamp waste was provided after mercury removal, and Hg was not detected by CV-AAS, this metal remained out of scope within the entire investigation.

Phosphor particle size was determined to majorly range between 2.75 and 8.70 µm (~60.8 %) (Fig. SM1, Supplementary material). With d_{10-}, d_{50-} and d_{90-} values of 2.42, 8.68 and 58.90 µm, respectively, the material was sufficiently dispersed to be suited for an efficient chlorination when in contact with the chlorinating agent $HCl_{(g)}$.

3.2. Preliminary tests and chlorination process

Prior to rotary kiln experiments, the reaction mixture was subjected to TGA/DTA analysis in order to characterize its thermochemical behavior in the investigated temperature range. The results are shown in Fig. SM2 (Supplementary material). The most characteristic peaks correspond to $NH_4Cl_{(s)}$ decomposition and REE chlorination: at T = 184ºC occurs phase transition to β-$NH_4Cl_{(s)}$ (Eq. (1)) followed by thermal decomposition, which initiates at $T \geq$ 220ºC (Eq. (2)) (Lorenz and Bertau, 2017) and reaches its maximum at T = 320ºC. This data is crucial for the process, since at higher temperatures NH_4Cl decomposition proceeds too fast. That in

turn results in excess gas volume causing higher flow velocity. As a consequence, the residence time of $HCl_{(g)}$ is too short as being displaced from the heating zone before the reaction can take place. To favor efficient chlorination (Eq. (3)) and reduce the $HCl_{(g)}$ volume, the experiments should be carried out in the above-given temperature range.

$$\propto -NH_4Cl_{(s)} \xrightarrow{\Delta} \beta - NH_4Cl_{(s)} \quad (1)$$

$$\beta - NH_4Cl_{(s)} \xrightarrow{\Delta} HCl_{(g)} + NH_{3(g)} \quad (2)$$

$$RE_2O_{3\,(s)} + 6\,HCl_{(g)} \rightarrow 2\,RECl_{3(s)} + 3\,H_2O_{(g)} \quad (3)$$

To define the factor ranges, preliminary tests were carried out. Regarding the $g_{NH4Cl}/g_{solidL1}$ ratio and the residence time ranges, SSC experiments were performed at 300 ºC. Upon increasing the NH_4Cl:$solid_{L1}$ ratio from 0.5 to 2, REE yields increase, too (Fig. 2.a). However, there is a slight decrease with 3 $g_{NH4Cl}/g_{solidL1}$. At first sight this appears contradictory, since higher $HCl_{(g)}$ availability should result in higher REE mobilization. The observation can easily be understood by taking a glance at the phosphor composition. While one major fraction is red phosphor YOX (Y_2O_3:Eu), another is blue phosphor ScAp ([Ca, Sr, Ba]$_5$(PO_4)$_3$Cl:Eu^{2+}). The answer is given by the fact that $HCl_{(g)}$ protonates ScAp upon which HPO_4^{2-} is released. This in turn forces Y^{3+} and Eu^{3+} to precipitate as insoluble $REPO_4$, what takes effect on the overall amount of released REE (Lorenz and Bertau, 2017). Therefore, NH_4Cl:$solid_{L1}$ ratios of 0.5, 1.0 and 1.5 were chosen for the DOE.

In contrast, phosphor residence time affects REE yield only slightly (Fig. 2.b). With marginal differences in yield between 90 and 120 min, there will be no significant effect on chlorination efficiency, but on operational costs. Therefore, residence time was chosen not to exceed 90 min in the DOE plan.

Fig. 2.c shows the strong impact of temperature on REE yields between 250 and 325 °C. With increasing temperature, REE yields increase, too, reaching their respective maximum at 80% (Eu) and 92% (Y) at 300 ºC. Temperatures exceeding 300 °C result in lower REE yields. In contrast to what was pointed out above, this effect is not owed to $REPO_4$ formation. Here, it is a consecutive reaction that interferes with SSC (Eq. 4). At $T \leq 300$ °C, Y_2O_3:Eu is chlorinated to give $RECl_{3(s)}$ which can be extracted by the leaching organic solution.

$$RE_2O_{3_{(s)}} \xrightarrow{HCl_{(g)}} RECl_{3(s)} \xrightarrow{HCl_{(g)}+NH_{4(g)}} NH_4RECl_{4_{(s)}} \quad (4)$$

However, longer residence time or higher temperature favor the second reaction to come into play. At longer residence times the effective exposure time to $NH_{3(g)}$ is higher, while at higher temperature there is a higher $NH_4Cl_{(s)}$ decomposition rate, what results in higher local partial pressures of $NH_{3(g)}$ and $HCl_{(g)}$. Both cases profit from the high initial surface of freshly formed $RECl_3$ through reacting with $NH_{3(g)}$ and $HCl_{(g)}$ to give $NH_4RECl_{4(s)}$, which is not extractable by the 2,4 pentanedione/ethanol mixture.

In order to demonstrate NH_4RECl_4 formation at 325 ºC, the chlorinated solids obtained at 300 ºC and 325 ºC, respectively, were analyzed by IR and XRD. The results are shown in Fig. 3. The spectrum shows the characteristic bands of the ammonium ion at $\tilde{\nu} = 2800$, 3000 and 3125 cm^{-1} (Borisov et al., 2011). The deformation of the ammonium ion in $NH_4Cl_{(s)}$ by the chloride ion is observed at $\tilde{\nu} = 1400$ cm^{-1} in both chlorinated solids. However, the peak is more significant for the solid chlorinated at 325 °C because in the chlorometal complex, the ammonium ion is associated with the larger species YCl_4^- and $EuCl_4^-$, what exceeds the deformation by the smaller NH_4^+ and results in a narrow and sharp peak (Borisov et al., 2011).

The weak peak at $\tilde{\nu} = 1060$ cm^{-1} is characteristic for ammonia in ammonium complexes (Oxton et al., 1975). This peak is not observed for the solid chlorinated at 300 °C, because the anionic species has not formed. The two weak peaks at $\tilde{\nu} =$ 580 and 773 cm^{-1} represent the chloride vibration in the tetrahedral ions ($RECl_4^-$). They are observed only for the solid chlorinated at 325 °C (Amiri and Shokrollahi, 2013; Mairesse et al., 2011).

Regarding XRD results, $YCl_{3(s)}$ and $NH_4Cl_{(s)}$ patterns are similar. The characteristic reflexes of both substances overlap, but the ammonium chloride is predominant in the samples obtained from SSC. Reflex intensities of $NH_4Cl_{(s)}$ (Chen et al., 2015) in the high temperature sample were lower owed to faster decomposition of $NH_4Cl_{(s)}$.

To corroborate the chlorination mechanism proposed in Eq. (4), two SSC experiments were performed. $NH_4Cl_{(s)}$ was mixed with synthetic $RE_2O_{3(s)}$ at a ratio of 1:1 and heated for 60 min. In fact, NH_4RECl_4 species were formed when SSC was carried out at 325 °C, and the products were not extractable with 2,4 pentanedione/ethanol mixture.

For these reasons, the chosen temperature levels were 260, 280 and 300 ºC, thus avoiding the undesired consecutive reaction (Eq. 4).

3.3. Box Behnken design

The 3^3 Box-Behnken design was chosen since it allows for examining the cross effects, which cannot be seen by varying one-factor-at-a-time. For instance, any change in reaction temperature results in two consequences: a shift to the chemical equilibrium and a change to the reaction rate at which the equilibrium is achieved. The latter always includes a correlation between temperature and time, which means that both can never be changed independently. DOE takes such correlations into account and they were therefore chosen as the best suited method to optimize the process.

This design requires experiments on every half of the edges and in the center. Experiments corresponding to the center point in Fig. SM3 (Supplementary material) were conducted in triplicate to determine the experimental error. The confidence interval was set to 95%. A multi-

linear regression was used to determine the regression parameters of all significant effects (Eq. (5)) to obtain the model equation describing how REE yields depend on each effect.

$$y = b_0 + \sum_{i=1}^{N} b_i x_i + \sum_{1 \le i \le j}^{N} b_{ij} x_i x_j + \sum_{i=1}^{N} b_{ii} {x_i}^2 \quad (5)$$

where:

y: Target value: REE yield

x_i*:* Factors: Temperature, residence time and $g_{NH4Cl}/g_{solidL1}$ ratio

N: Number of factors (3)

b_0*:* Ordinate section

b_i, b_{ij}, b_{ii}*:* Regression parameters of linear, squared, and cross effects

3.4. Optimization

To get the model optimization equation of both REE yields, Eq. (5) was used to investigate the nine effects (linear, squared, and binary correlations) which can influence the yield. The Pareto diagram (Fig. 4.a) shows that seven of nine effects are significant. Only the AB and BC binary correlations are insignificant to the Y yield optimization and, therefore both correlations were removed from Eq. (5) by the stepwise method.

As expected, temperature has the greatest effect on Y yield, followed by the $g_{NH4Cl}/g_{solidL1}$ ratio. Residence time has the least influence on Y yield, because the reaction is almost completed after 30 min (Lorenz and Bertau, 2019). AC correlation is the only significant cross effect, which is easily understood in terms of temperature and reactant concentration affecting the equilibrium. AB and BC binary correlations are insignificant for both Y and Eu yield. They were removed by the stepwise method. Although the Eu optimization results are similar to the ones from Y, some differences can be observed (Fig. 4.b). For instance, the temperature and the AA cross effect have less influence for Eu than for Y. This is mainly explained by the different concentrations of both metals in the solid treated. Whether or not different chemical properties of both metals are involved, too, can neither be excluded nor confirmed. Yet, in view of the rather minor Eu content, such effects will be rather subordinate.

3.5. Model equations and optimum

The model equations allow for predicting the REE yields at any desired point within the examined factors value range, what minimizes optimization efforts for the REE recovery process.

The final Y model equation (Eq. (6)) predicts 95.7% as a maximum yield for these reaction conditions: 295.9 °C, 67 min and 1.27 $g_{NH4Cl}/g_{solidL1}$. An experiment with these parameters was carried out in duplicate to validate the model. Both experiments gave a global optimum of

94.9 ± 0.8% (Table SM3, Supplementary material). The Y-model optimization has been validated obtaining a coefficient of determination $R^2 = 0.9953$.

$$Y_{yield}(\%) = -5076.04 + 35.0526 \cdot A + 1.33439 \cdot B - 90.9237 \cdot C - 0.0612 \cdot A^2 + 0.9156 \cdot A \cdot C - 0.0099 \cdot B^2 - 70.1363 \cdot C^2 \quad (6)$$

$$Eu_{yield}(\%) = -4661.69 + 32.3075 \cdot A + 1.41159 \cdot B - 140.772 \cdot C - 0.0567 \cdot A^2 + 0.9984 \cdot A \cdot C - 0.0105 \cdot B^2 - 52.6316 \cdot C^2 \quad (7)$$

where:

A: Temperature (°C)

B: Residence time (min)

C: Ratio ($g_{NH4Cl}/g_{solidL1}$)

The model equation for Eu optimization is shown in Eq. (7). The maximum yield, which was estimated to amount to 96.6%, can be reached at 298.1 °C, 67 min and 1.49 $g_{NH4Cl}/g_{solidL1}$. The model was also validated in duplicate experiments. In contrast to Y, though, Eu yield does not reach its maximum under these conditions. With $R^2 = 0.9864$ the value is somewhat lower than the one obtained for Y, nevertheless it is shown how well the results are replicated by the model. Under the optimal Y reaction conditions, Eu yield was 92.2 ± 1.9% (Table SM3. Supplementary material), what is only 4.6 % less than the predicted maximum value.

The recovery yields obtained here are in line with a recent report by Cenci et al., who separated > 95.2% of Ga, Ce and Y from waste LED by physical processes (Cenci et al., 2021). However, there are rather marked differences, when Eu and Y were recovered from cathode ray tubes (CRT) phosphors. With pyrophosphate as a complexing agent yields did not exceed 90 for Y and 58% for Eu (Alvarado-Hernández et al., 2019). Once it has been shown that both REE are recoverable from CRT phosphors, SSC coupled with selective organic leaching appears as an interesting option to reach higher REE yields.

Considering a technical application of this process, the economic optimum is decisive, i.e. the process has to bridge the gap between least possible chemicals costs and highest possible REE yield. The economic optimum was achieved by reducing the $g_{NH4Cl}/g_{solidL1}$ ratio by 54% from 1.27 to 0.58 with all other parameters remaining unaltered. In this case, total REE yield dropped by 35.3 % from 92.0 to 59.5% (Reduced optimum in Table SM4, Supplementary material), what is clearly a compromise between minimizing costs and maximizing yields.

3.6. Leaching solution optimization

The organic extractant composed of 2,4-pentanedione and ethanol serves to extract the REE chlorides from the crude SSC reaction mixture. The concept was, that the trivalent REE cations

form a tridentate complex with the diketone, while ethanol acts as a solvent for both excess pentanedione and the REE complex. Accompanying metal chlorides however do not form complexes with the organic extractant, for which reason this approach is a superior to conventional leaching with aqueous (buffered) systems. After leaching, as expected > 99% of the REE were transferred into the organic phase (Table SM5. Supplementary material). The amount of extractant yet had to be optimized since the leaching solution (50 mL, 10% 2,4-pentanedione) was added in excess (Eq. (8)) at the beginning to ensure complete complexation. In the following, different experiments were done varying L:S ratios.

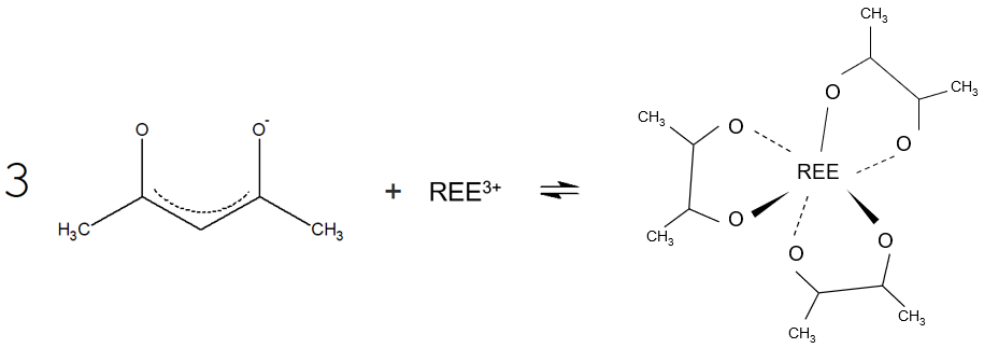

(8)

The solid was a mixture of 1 g of the $solid_{L1}$ and 1.27 g of $NH_4Cl_{(s)}$, what represents the solid composition after the crude SSC reaction mixture obtained from the optimized process had cooled down to ambient temperature. Being incapable of forming complexes with 2,4-pentanedione the surplus of $NH_4Cl_{(s)}$ does not interfere with the extraction process. Moreover, after removing volatile remnants, it can be reused in the next SSC run, thus contributing to overall process economy. In a nutshell, the amount of leaching solution was significantly reduced to almost its half obtaining the same REE yields (Table SM6. Supplementary material), being 30 mL the optimal volume for the 2,4-pentanedione/ethanol mixture.

3.7. Comparison to acid leaching and future research

Prior to developing the process described here, intensive research activities have been underway. With the exception of the SepSELSA process all of them were based on wet acid leaching. In order assess process efficiency and to roughly estimate process economy of this new process it has been compared with the one reported by Pavón et al. (Pavón et al., 2019, 2018) (Fig. SM4, Supplementary material). The starting material considered for comparison was the unreacted solid residue obtained after magnetic separation, HNO_3 leaching and filtration of fluorescent lamp waste.

The classical approach foresees a second HNO_3 leaching as first process step. If this is replaced by SSC, the number of process steps to obtain a REE pregnant solution is reduced by 3, since pH adjustment, oxalate precipitation to separate REE from non-REE and redissolution have become obsolete. Furthermore, $NH_{3(g)}$ is produced in stoichiometric amounts from $NH_4Cl_{(s)}$ compared to the amount of $HCl_{(g)}$ consumed in the SSC reaction,

providing the option of selling it as a co-product. The 2,4-pentanedione/ethanol mixture extracts the SSC crude product selectively for REE chlorides. The last step is obtaining an aqueous REE solution, which is achieved by removing the volatile components at elevated temperature (> 90 °C) and adding of HNO_3. 2,4-pentanedione and ethanol can be reused in the process.

The wet acid leaching process employs 3.22 tons of chemicals for 1 ton of REE (Table SM7, Supplementary material), whereas the SSC conducted with global optimum parameters consumes only 1.30 tons. Conceivably, the SSC process can be considered greener than classic wet acid treatment, not only owed to the reduced chemicals consumption. Depending on whether global or reduced optimum parameters are applied, there a considerable reduction of 59% or 81%, respectively. The commodity chemicals prices used for the economic comparison are summarized in Table SM8 (Supplementary material). The costs were determined to produce 1 ton of REE considering whether NH_3 is sold (co-product) or not. Without selling NH_3 as a product, the chemicals costs by using SSC are 1,558 €. However, for the wet acid leaching process, 10,172 € are spent (Fig. SM5, Supplementary material). Consequently, SSC allows for reducing the expenses by 85%. As a particular benefit, chemicals costs are fully compensated for when NH_3 solution is marketed, eventually yielding a profit of 2,660 €.

The operating costs including chemicals and energy consumption for the wet acid leaching process are 10,172 € (Fig. 5). By using the SSC process operating with the global optimum parameters and without selling the NH_3 solution, a saving of 201 € can be achieved, resulting in total costs of 9,971 €. Using the reduced optimum parameters, the total costs are even lower. They are reduced to 598 and 397 € compared to the wet acid leaching process. Considering NH_3 as a co-product, the total costs using global optimum parameters are reduced to 5,752 €. 6,375 € are the costs using the reduced optimum parameters. Taking into account that the costs without selling NH_3 solution are considered without $NH_4Cl_{(s)}$ recirculation, the chemicals consumption was determined in a conservative scenario (Lorenz and Bertau, 2019).

In order to reduce energy consumption in distillative organic extractant removal, other options to recirculate the solution can be studied, e.g., REE precipitation with $NaOH_{(s)}$ and filtration. Further research is required to develop completely the REE recovery process obtaining Y and Eu in an oxide form. The obtained REE liquor as a product of the suggested current process can be treated by solvent extraction processes to individually separate both REE (G. D. Saratale et al., 2020). By established processes such as oxalic acid precipitation and calcination, Y_2O_3 and Eu_2O_3 are obtained. Furthermore, to the best of our knowledge, the SepSELSA process operated by FNE Entsorgungsdienste Freiberg GmbH, Freiberg, Germany is the first implementation of an unconventional SSC process on an industrial scale.

Building upon the results of this study, follow-up work aims at further optimizing this process to keep on commercial REE recycling from lamp phosphors going despite low REE prices.

4. Conclusions

REE recovery process from fluorescent lamp waste has been improved significantly by applying the SSC process and REE-selective organic leaching. The empirical models generated by using a DOE 3^3 Box-Behnken, describe how REE yields depend on temperature, residence time and $g_{NH4Cl}/g_{solidL1}$ ratio. As a result, 95.7% of Y and 92.2% of Eu can be recovered selectively at optimum parameters of 295.9 °C, 67 min and a ratio of 1.27 of $g_{NH4Cl}/g_{solidL1}$. The overall REE yield under global optimum parameters was 92.0 %. Regarding the leaching stage, the organic mixture of 2,4-pentanedione diluted in ethanol has been proven an effective alternative for REE separation, because of its high discriminative power towards non-REE metals. The resulting process profits from less process steps, since neutralization, precipitation and re-dissolution are no longer required. As a result, chemicals consumption and costs are reduced by up to 85% compared to wet acid treatment. Furthermore, excess NH_3 can be marketed as a solution, even over-compensating for the chemicals costs. Improving the cost-intensive recirculation of the organic mixture remains a challenge and is a matter of consecutive work to optimize energy consumption. Despite high energy costs, the process described here is considerably more cost-efficient compared to existing approaches. In summary, this process achieves lamp waste valorization through an economical alternative to fluorescent lamp wastes management achieving almost complete REE recycling, thus not only inverting costs into revenues, but also contributing to securing the raw material base.

Acknowledgment

This investigation was partially supported by MINECO [grant number CRM2017-83581-R]. We express our gratitude to Recyberica Ambiental S.L for providing free fluorescent lamp wastes samples. Further thanks are owed to Andrea Schneider and Dr. Sebastian Hippmann, Institute of Chemical Technology for conducting ICP-OES and TGA/DTA analyses, and Dr. Juan Francisco Miñambres, Institute of Physical Chemistry, for conducting XRD analysis. Additional thanks go to Martin Seifert, FNE Entsorgungsdienste Freiberg GmbH, Freiberg, Germany, for providing economical data and helpful discussions.

References

Ahn, N.K., Shim, H.W., Kim, D.W., Swain, B., 2020. Valorization of waste NiMH battery through recovery of critical rare earth metal: A simple recycling process for the circular economy. Waste Manag. 104, 254–261. https://doi.org/10.1016/j.wasman.2020.01.014

Alvarado-Hernández, L., Lapidus, G.T., González, F., 2019. Recovery of rare earths from waste cathode ray tube (CRT) phosphor powder with organic and inorganic ligands. Waste Manag. 95, 53–58. https://doi.org/10.1016/j.wasman.2019.05.057

Amiri, S., Shokrollahi, H., 2013. Magnetic and structural properties of RE doped Co-ferrite (RE=Nd, Eu, and Gd) nano-particles synthesized by co-precipitation. J. Magn. Magn. Mater. 345, 18–23. https://doi.org/10.1016/j.jmmm.2013.05.030

Bertau, M., Fröhlich, P., Jacob-Seifert, K., Seifert, M., 2015. Vorrichtung und Verfahren zur Abtrennung und Konzentration von Bestandteilen mit magnetischem Verhalten aus einer ionenhaltigen Lösung. DE102014211289 (A1).

Bertau, M., Fröhlich, P., Lorenz, T., 2014. Verfahren zur Rückgewinnung Seltener Erden aus Seltene Erden-haltigen Leuchtstoffen. DE102014224015 B4.

Borisov, V.A., D'yachenko, A.N., Kraidenko, R.I., 2011. Reaction of ammonium chloride with the copper(II) sulfide and oxide, and identification of the reaction products. Russ. J. Gen. Chem. 81, 1430–1433. https://doi.org/10.1134/S107036321107005X

Cenci, M.P., Dal Berto, F.C., Camargo, P.S.S., Veit, H.M., 2021. Separation and concentration of valuable and critical materials from wasted LEDs by physical processes. Waste Manag. 120, 136–145. https://doi.org/10.1016/j.wasman.2020.11.023

Chen, H., Wang, J., Hou, S., Xiang, L., 2015. Influence of NH4Cl on hydrothermal formation of α-CaSO4·0.5H2O Whiskers. J. Nanomater. 2015, 0–7. https://doi.org/10.1155/2015/670872

Forti, V., Baldé, C.P., Kuehr, R., Bel, G., 2020. The Global E-waste Monitor 2020: Quantities, Flows, and the Circular Economy Potential, United Nations University (UNU)/United Nations Institute for Training and Research (UNITAR) – co-hosted SCYCLE Programme, International Telecommunication Union (ITU) & International Solid Waste Association (ISWA), Bonn/Geneva/Rotterdam.

Gutiérrez-Gutiérrez, S.C., Coulon, F., Jiang, Y., Wagland, S., 2015. Rare earth elements and critical metal content of extracted landfilled material and potential recovery opportunities. Waste Manag. 42, 128–136. https://doi.org/10.1016/j.wasman.2015.04.024

Hasegawa, H., Begum, Z.A., Murase, R., Ishii, K., Sawai, H., Mashio, A.S., Maki, T.,

Rahman, I.M.M., 2018. Chelator-induced recovery of rare earths from end-of-life fluorescent lamps with the aid of mechano-chemical energy. Waste Manag. 80, 17–25. https://doi.org/10.1016/j.wasman.2018.08.049

Innocenzi, V., De Michelis, I., Kopacek, B., Vegliò, F., 2014. Yttrium recovery from primary and secondary sources: A review of main hydrometallurgical processes. Waste Manag. 34, 1237–1250. https://doi.org/10.1016/j.wasman.2014.02.010

Li, J., Li, M., Zhang, D., Gao, K., Xu, W., Wang, H., Geng, J., Huang, L., 2020. Clean production technology of Baiyun Obo rare earth concentrate decomposed by Al(OH)3-NaOH. Chem. Eng. J. 382, 122790. https://doi.org/10.1016/j.cej.2019.122790

Li, L., Hu, J. hang, Wang, H., 2018. Application of the chloridizing roasting method for the removal of copper and sulphur from copper slags. Miner. Process. Extr. Metall. Trans. Inst. Min. Metall. 127, 49–55. https://doi.org/10.1080/03719553.2017.1288357

Lorenz, T., Bertau, M., 2020. Recycling of rare earth elements from SmCo5-Magnets via solid-state chlorination. J. Clean. Prod. 246, 118980. https://doi.org/10.1016/j.jclepro.2019.118980

Lorenz, T., Bertau, M., 2019. Recycling of rare earth elements from FeNdB-Magnets via solid-state chlorination. J. Clean. Prod. 215, 131–143. https://doi.org/10.1016/j.jclepro.2019.01.051

Lorenz, T., Bertau, M., 2017. Recycling of Rare Earth Elements. Phys. Sci. Rev. https://doi.org/10.1515/psr-2016-0067

Lorenz, T., Golon, K., Fröhlich, P., Bertau, M., 2015. Rückgewinnung Seltener Erden aus quecksilberbelasteten Leuchtstoffen mittels Feststoffchlorierung. Chemie Ing. Tech. 87, 1373–1382. https://doi.org/10.1002/cite.201400181

Mairesse, G., Barbier, P., Wignacourt, J.-P., Rubbens, A., Wallart, F., 2011. X-Ray, Raman, infrared, and nuclear magnetic resonance studies of the crystal structure of ammonium tetrachloroaluminate, NH4AlCl4. Can. J. Chem. 56, 764–771.

Mu, W., Cui, F., Xin, H., Zhai, Y., Xu, Q., 2020. A novel process for simultaneously extracting Ni and Cu from mixed oxide-sulfide copper-nickel ore with highly alkaline gangue via FeCl3·6H2O chlorination and water leaching. Hydrometallurgy 191, 105187. https://doi.org/10.1016/j.hydromet.2019.105187

Okabe, P., Newton, M., Rappleye, D., Simpson, M.F., 2020. Gas-solid reaction pathway for chlorination of rare earth and actinide metals using hydrogen and chlorine gas. J. Nucl. Mater. 534, 152156. https://doi.org/10.1016/j.jnucmat.2020.152156

Oxton, I.A., Knop, O., Falk, M., 1975. Infrared Spectra of the Ammonium Ion in Crystals. I.

518 Ammonium Hexachloroplatinate(IV) and Hexachlorotellurate(IV). Can. J. Chem. 53,
519 2675–2682.

520 Park, H.S., Rhee, S.W., 2016. Estimation of retorted phosphor powder from spent
521 fluorescent lamps by thermal process. Waste Manag. 50, 257–263.
522 https://doi.org/10.1016/j.wasman.2016.01.032

523 Pavón, S., Fortuny, A., Coll, M.T., Sastre, A.M., 2019. Improved rare earth elements
524 recovery from fluorescent lamp wastes applying supported liquid membranes to the
525 leaching solutions. Sep. Purif. Technol. 224, 332–339.
526 https://doi.org/10.1016/j.seppur.2019.05.015

527 Pavón, S., Fortuny, A., Coll, M.T., Sastre, A.M., 2018. Rare earths separation from
528 fluorescent lamp wastes using ionic liquids as extractant agents. Waste Manag. 82,
529 241–248. https://doi.org/10.1016/j.wasman.2018.10.027

530 Saratale, G.D., Kim, H.Y., Saratale, R.G., Kim, D.S., 2020. Liquid–liquid extraction of yttrium
531 from the sulfate leach liquor of waste fluorescent lamp powder: Process parameters and
532 analysis. Miner. Eng. 152, 106341. https://doi.org/10.1016/j.mineng.2020.106341

533 Saratale, R.G., Kim, H.Y., Park, Y., Shin, H.S., Ghodake, G., Bharagava, R.N., Mulla, S.I.,
534 Kim, D.S., Saratale, G.D., 2020. Hydrometallurgical process for the recovery of yttrium
535 from spent fluorescent lamp: Leaching and crystallization experiments. J. Clean. Prod.
536 261, 121009. https://doi.org/10.1016/j.jclepro.2020.121009

537 Su, X., Wang, Y., Guo, X., Dong, Y., Gao, Y., Sun, X., 2018. Recovery of Sm(III), Co(II) and
538 Cu(II) from waste SmCo magnet by ionic liquid-based selective precipitation process.
539 Waste Manag. 78, 992–1000. https://doi.org/10.1016/j.wasman.2018.07.004

540 Swain, N., Mishra, S., 2019. A review on the recovery and separation of rare earths and
541 transition metals from secondary resources. J. Clean. Prod.
542 https://doi.org/10.1016/j.jclepro.2019.02.094

543 U.S. Geological Survey, 2020. Mineral Commodity Summaries 2020, United States
544 Geological Survey.

545 Wu, S., Wang, L., Zhao, L., Zhang, P., El-Shall, H., Moudgil, B., Huang, X., Zhang, L., 2018.
546 Recovery of rare earth elements from phosphate rock by hydrometallurgical processes
547 – A critical review. Chem. Eng. J. 335, 774–800.
548 https://doi.org/10.1016/j.cej.2017.10.143

549 Xing, Z., Cheng, G., Yang, H., Xue, X., Jiang, P., 2020. Mechanism and application of the
550 ore with chlorination treatment: A review. Miner. Eng. 154, 106404.
551 https://doi.org/10.1016/j.mineng.2020.106404

552 Yang, D., Gao, S., Hong, J., Ye, L., Ma, X., Qi, C., Li, X., 2019. Life cycle assessment of rare
553 earths recovery from waste fluorescent powders – A case study in China. Waste
554 Manag. 99, 60–70. https://doi.org/10.1016/j.wasman.2019.08.038

555 Yu, M., Pang, S., Mei, G., Chen, X., 2016. Recovering Y and Eu from waste phosphors using
556 chlorination roasting—water leaching process. Minerals 6, 1–12.
557 https://doi.org/10.3390/min6040109

558

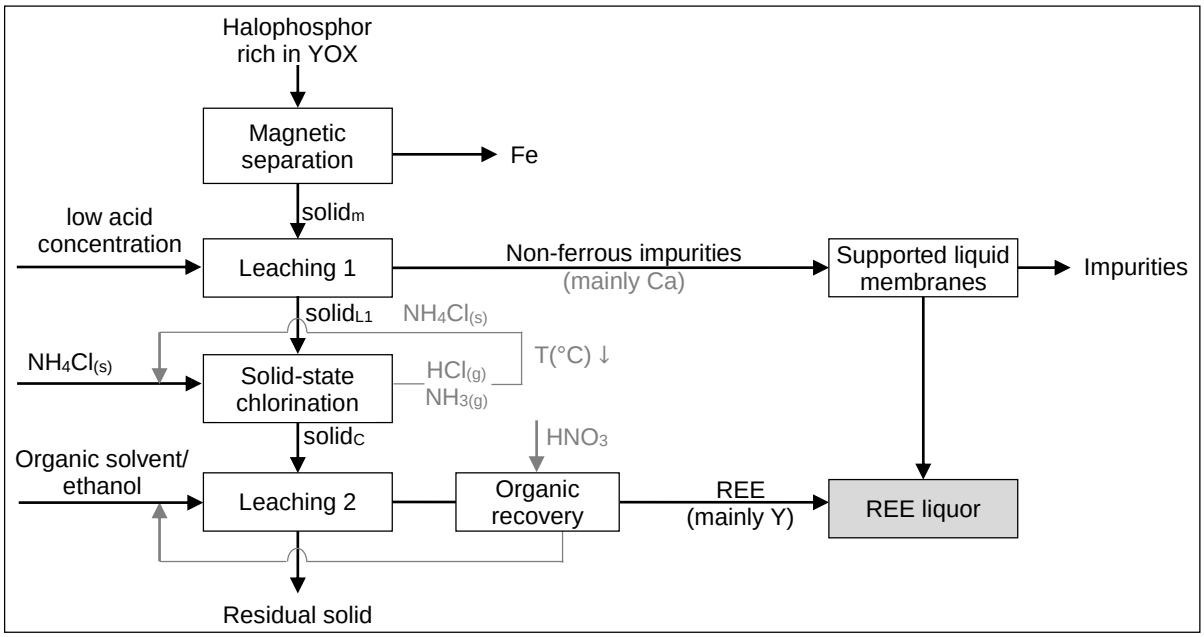

559

560 **Fig. 1.** Flowsheet of the REE recovery process from YOX fluorescent lamp wastes introducing
561 the SSC stage using organic mixture as leaching solution.

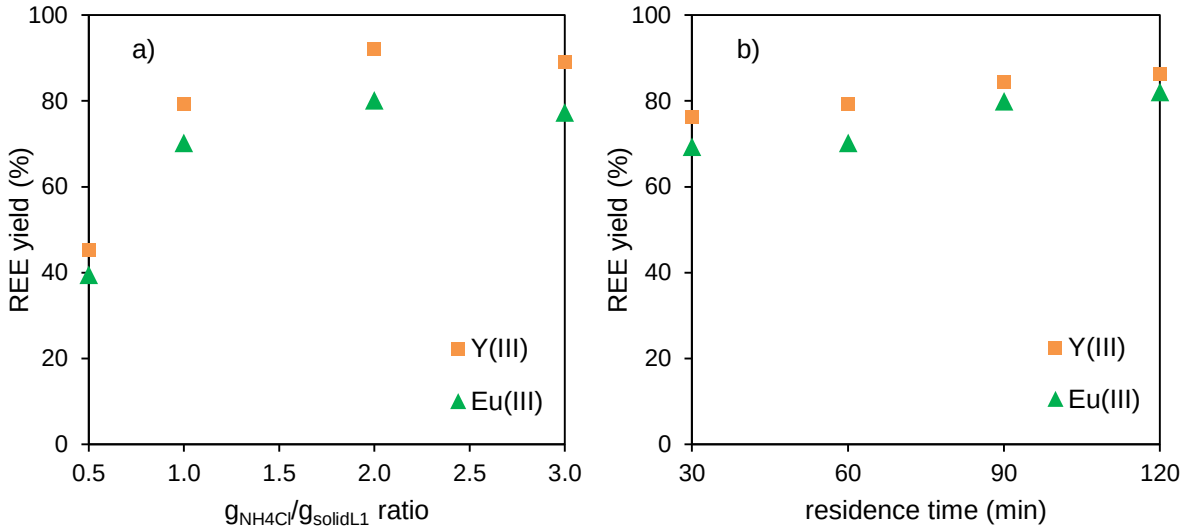

562

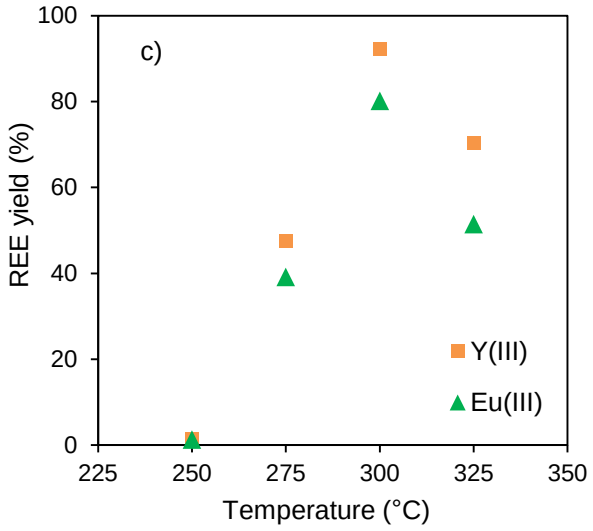

563

564 **Fig. 2.** Effect of the chlorination factors on the REE yields. a) 300 ºC, 60 min varying the ratio
565 from 0.5 to 3. b) 300 ºC, 1 $g_{NH4Cl}/g_{solidL1}$ varying the residence time from 30 to 120 min. c)
566 60 min, 1 $g_{NH4Cl}/g_{solidL1}$ and a temperature range from 250 to 350 ºC.

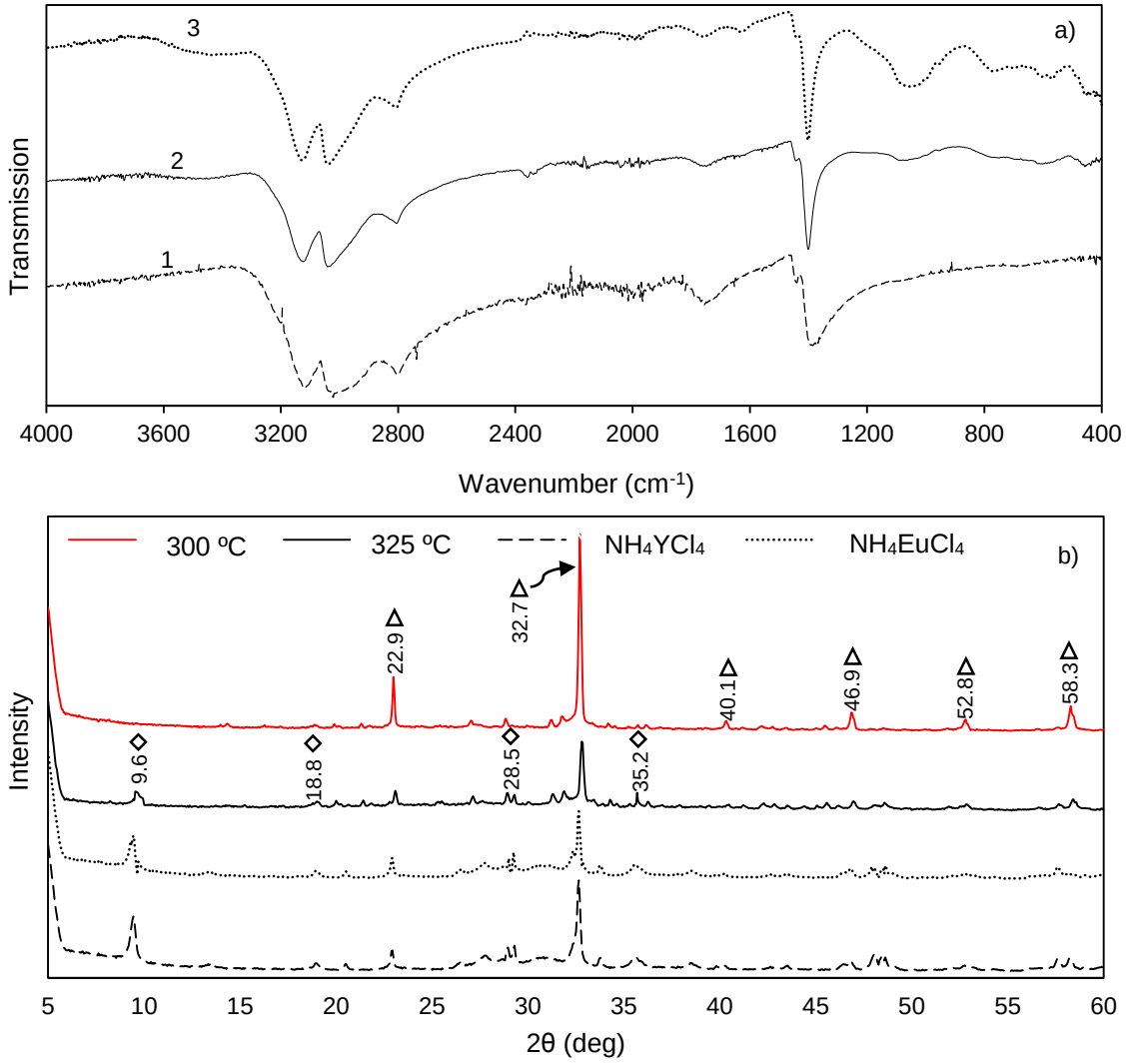

Fig. 3. a) IR spectra of (1) $NH_4Cl_{(s)}$ (2) solid chlorinated at 300 °C (3) solid chlorinated at 325 °C. b) XRD patterns for $solid_{L1}$ chlorinated at 300 ºC and 325 °C, and solid chlorinated using RE_2O_3 as raw oxides at 325 ºC. (◇) NH_4RECl_4, (△) NH_4Cl.

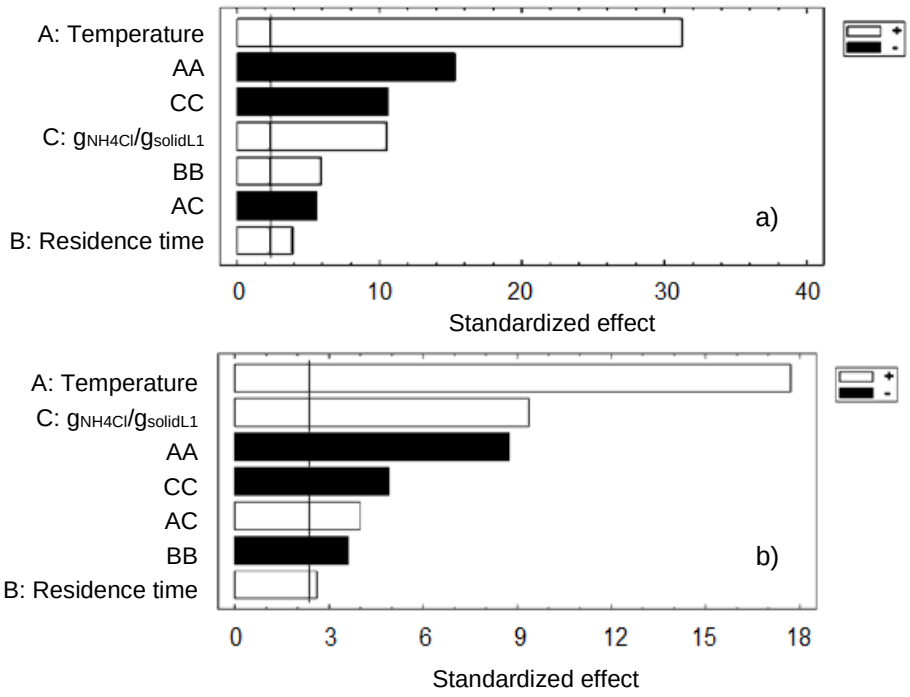

Fig. 4. Pareto diagram with all the effects influencing REE yield (black line refers to experimental error). a) Y. b) Eu

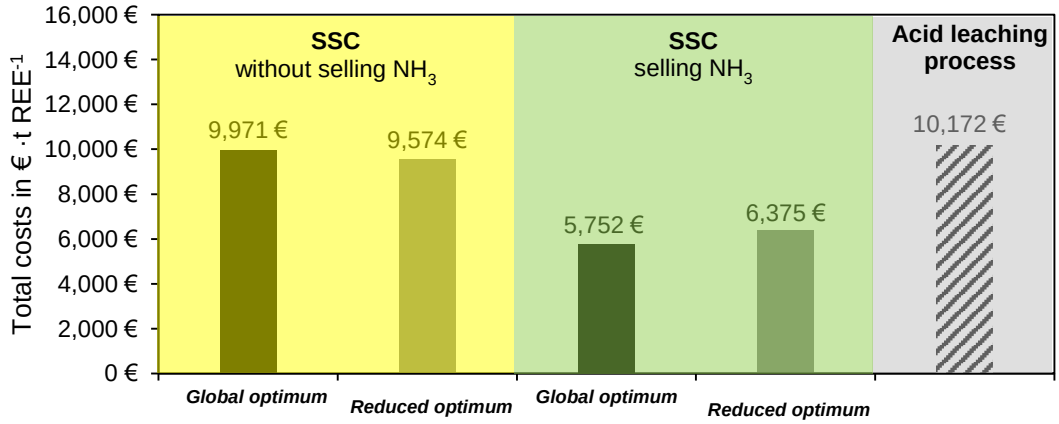

585

586 **Fig. 5.** Comparison of chemicals and energy costs using SSC and acid leaching processes
587 operated at global and reduced optimum parameters.

588 **Table 1.** 3^3 Box-Behnken design (A: Temperature; B: Residence time; C: ratio of $g_{NH4Cl}/g_{solidL1}$).

589 The experiments shaded in grey correspond to the replicated central point.

Nr.	Factors			Levels			Y_{yield} (%)	Eu_{yield} (%)
	A (°C)	B (min)	C ($g_{NH4Cl}/g_{solidL1}$)	A	B	C		
1	280	60	1.0	0	0	0	79.3	74.1
2	280	30	0.5	0	-1	-1	38.7	30.9
3	260	30	1.0	-1	-1	0	3.3	2.9
4	300	90	1.0	1	1	0	84.3	83.5
5	280	90	0.5	0	1	-1	44.9	37.1
6	280	90	1.5	0	1	1	70.9	75.1
7	260	60	0.5	-1	0	-1	3.0	5.6
8	280	60	1.0	0	0	0	78.7	73.8
9	300	60	1.5	1	0	1	88.5	89.8
10	280	30	1.5	0	-1	1	58.0	64.7
11	300	30	1.0	1	-1	0	78.5	70.3
12	260	60	1.5	-1	0	1	6.7	15.4
13	260	90	1.0	-1	1	0	14.8	10.7
14	300	60	0.5	1	0	-1	49.0	41.0
15	280	60	1.0	0	0	0	78.05	73.5

590

591 **Table 2**. Average element content in the solid$_{L1}$. Aqua regia leaching (90 ± 2 °C, 2 h).

	Element	$g_{metal}/kg_{solid\ L1}$
REE	Y	111.8 ± 0.9
	Eu	8.0 ± 0.2
	Ce	1.5 ± 0.2
	Gd	1.5 ± 0.1
	La	1.4 ± 0.2
Non-REE	Ca	10.5 ± 0.8
	P	5.3 ± 0.4
	Na	2.9 ± 0.3
	Sr	1.5 ± 0.1
	Ba	1.1 ± 0.06
	Mg	0.8 ± 0.06
	Sb	0.7 ± 0.04
	K	0.3 ± 0.03
	Mn	0.2 ± 0.02
	Fe	0.2 ± 0.05
	Hg	n.d.
Total REE		**124.3 ± 2**

592